
Debiasing Vision-Language Models via Biased Prompts

Ching-Yao Chuang[†], Varun Jampani[‡], Yuanzhen Li[‡],
Antonio Torralba[†] Stefanie Jegelka[†]
[†]MIT CSAIL, [‡]Google Research
{cychuang, torralba, stefje}@mit.edu
{varunjampani, yzli}@google.com

Abstract

Machine learning models have been shown to inherit biases from their training datasets. This can be particularly problematic for vision-language foundation models trained on uncurated datasets scraped from the internet. The biases can be amplified and propagated to downstream applications like zero-shot classifiers and text-to-image generative models. In this study, we propose a general approach for debiasing vision-language foundation models by projecting out biased directions in the text embedding. In particular, we show that debiasing only the text embedding with a calibrated projection matrix suffices to yield robust classifiers and fair generative models. The proposed closed-form solution enables easy integration into large-scale pipelines, and empirical results demonstrate that our approach effectively reduces social bias and spurious correlation in both discriminative and generative vision-language models without the need for additional data or training. The code is available at https://github.com/chingyaoc/debias_v1.

1 Introduction

Foundation vision-language models, such as CLIP [33], DALLE-2 [35], Imagen [38], and Stable Diffusion [36], which are trained on extensive multimodal data at a massive scale, have led to a significant shift in the landscape of machine learning systems. Specifically, contrastive vision-language encoders like CLIP have the ability to perform zero-shot inferences without fine-tuning, and language embeddings can be used to train high-quality text-to-image models [36].

While vision-language models demonstrate impressive capabilities, it is important to recognize that they may also exacerbate biases [28, 1, 42]. Recent studies [4] have shown that the datasets these models are trained on can contain inappropriate image-text pairs with stereotypes, racist content, and ethnic slurs. The biases are then propagated to downstream applications [1, 42], resulting in biased predictions. In addition to social biases, zero-shot models derived from vision-language models can also suffer from more general forms of spurious correlations such as image background, leading to poor group robustness [49]. Biases also exist in generative models, where generated images may exhibit bias towards certain genders and races [7, 29]. Substantial progress has been made recently toward mitigating biases in vision-language models [32, 3, 49]. However, many current approaches for addressing bias in models require training or fine-tuning the models using resampled datasets or modified objectives, which can be computationally intensive for foundation models.

In this work, we propose a general approach for self-debiasing foundation vision-language models by projecting out biased directions in the text embedding. Given a vision-language encoder such as CLIP, we define a set of biased directions in the embedding using prompts that describe the biases. For instance, prompts like “a photo of a male/female” define a biased subspace in the latent space. One approach to mitigating these biases is to construct a projection matrix, a linear transformation of

the text embedding that projects out the biased directions [6]. However, solely relying on prompts to define biased directions may be unstable and noisy [15]. To address this issue, we propose a calibration loss that minimizes the discrepancy of a pair of prompt embeddings. For example, given a projection matrix that removes gender information, the projected vectors of prompts “a photo of a male doctor” and “a photo of a female doctor” should be similar. Based on this principle, we design an objective to calibrate the projection matrix, which has an easily solvable closed-form solution. This allows for the construction of the projection matrix to be *training-free and requires no downstream dataset or labels*, making it suitable for large-scale models. Empirically, we find that debiasing only the text embedding with a calibrated projection matrix suffices to improve the group robustness of zero-shot models on well-established benchmarks.

We then extend our approach to generative models such as Stable Diffusion [36], a widely adopted text-to-image model conditioned on text embeddings from CLIP [33]. The inherent challenge lies in the fact that generative models are distinctly dissimilar from zero-shot classification, where the target classes are explicitly defined. With generative models, our objective is to develop a debiasing matrix that is universally applicable to every prompt. This matrix can then be employed as a standard preprocessing stage prior to feeding the text embedding into the generative model. To accomplish this, we solve the calibration matrix with a set of positive pairs which comprise various prompts from the training dataset, and debias the unseen prompts with the obtained matrix. Similar to debiasing zero-shot models, the projection matrix improves the diversity of generated images from text-to-image models without altering the model parameters.

In short, this work makes the following contributions:

- We present a simple and general approach for debiasing vision-language models;
- The proposed approach does not require training, data, or labels, making it computationally efficient for use with foundation models;
- We evaluate our approach through experiments on both discriminative (zero-shot, text-image retrieval) and generative (diffusion) vision-language models.

2 Related Works

Vision-Language models [33, 35, 38, 36] have become increasingly widespread in recent years. However, these models are known to suffer from spurious correlations and can be biased towards certain races and gender. Birhane et al. [4] study the datasets these models are trained on and show that their biases can be inherited by the models. Various methods have been proposed to address biases, but many of them only address single-modality models.

Biases in Language Models Large-scale language models have been shown to contain harmful or misrepresentative biases [5, 30, 46]. Previous research has demonstrated the presence of gender bias in natural language processing systems [6, 51] as well as racial bias [27, 13]. Bolukbasi et al. [6] first proposed the use of orthogonal projections to remove gender biases in word embeddings. This approach was later extended to debiasing sentence embeddings [24]. Alternative methods include regularizing the models with constraints on training data [50, 19] or directly modifying the dataset [40, 51]. However, scaling these approaches to large foundation models can be challenging as they often require retraining the backbone encoders.

Biases in Vision Models Gender and racial biases have also been widely explored in computer vision [2, 43], in terms of discriminative models [44] and generative models [48, 16, 7]. Many debiasing approaches aim to learn good representations via adversarial training [26, 45], or augmenting the biased dataset [34, 9]. Beyond social bias, many works study spurious correlations, a more general form of bias that can include features such as image background or other non-target attributes that are correlated with labels. This problem of spurious correlations is often studied and tackled as a group robustness problem [37, 20]. Kirichenko et al. [22] show that last layer re-training is sufficient for robustness to spurious correlations, which aligns with our finding that debiasing the zero-shot weights suffices to yield robust classifiers.

Biases in Vision-Language Models Recently, biases in multimodal settings have gained significant attention [1, 17]. Wang et al. [42] propose to remove dimensions in the CLIP embedding that are highly correlated with gender attributes. Berg et al. [3] debias the CLIP models with prompt learning

via an adversarial approach. Seth et al. [39] learn additive residual image representations to offset the biased representations. Recently, Zhang and Ré [49] address the group robustness of vision-language models with contrastive learning. These previous works are data-oriented, where models are trained or finetuned on labeled datasets. In contrast, our approach is fully zero-shot, which does not require any downstream dataset and model training. To debias generative models, a recent work [11] pre-defines a look-up table to provide fair guidance for text-to-image diffusion models. Nevertheless, this method encounters limitations when faced with previously unseen classes that are absent from the look-up table, while our approach generalizes well to new concepts.

3 Biases and Spurious Correlations

We consider a dataset in which each input $x \in \mathcal{X}$ is associated with multiple attributes, including the target class $y \in \mathcal{Y}$ and a spurious attribute $a \in \mathcal{A}$. We focus on the case where biases are present and the attribute a is spuriously correlated with the label y . For instance, the class “doctor” could be correlated with the spurious attribute “gender” in the datasets foundation models are trained on [4]. Importantly, these biases can be transferred to downstream tasks, both discriminative and generative.

Discriminative Models In this work, we examine the biases present in zero-shot classifiers obtained via a vision-language encoder such as CLIP. These classifiers are built by assigning each row of the linear classifier weight $\beta \in \mathbb{R}^{K \times d}$ to be the embedding of a “class prompt”, for example, “a photo of a [class name]” [33]. Importantly, it does not require any data or training to construct these zero-shot classifiers. However, it is possible for these zero-shot classifiers to inherit biases from the dataset used to train the vision-language models. To study these biases, we utilize the group robustness framework proposed by Sagawa et al. [37]. In this setting, groups are defined by a combination of the labels and spurious attributes: $\mathcal{G} \in \mathcal{Y} \times \mathcal{A}$. Given a distribution P_g conditioned on $g \in \mathcal{G}$ and a loss function $\ell : \mathcal{Y} \times \mathcal{Y} \rightarrow \mathbb{R}$, group robustness requires that the classifier $f : \mathcal{X} \rightarrow \mathcal{Y}$ achieves a small gap between its worst-group error and average error:

$$\max_{g \in \mathcal{G}} \mathbb{E}_{x, y \sim P_g} [\ell(f(x), y)] - \mathbb{E}_{x, y \sim P} [\ell(f(x), y)]. \quad (1)$$

The definition of metrics for text-image retrievals, such as maximal skewness [14], will be deferred to the experiment section.

Generative Models A text-to-image model learns a conditional distribution $\hat{P}(X|Z = z)$, where z is the embedding of the prompt. However, the biased nature of the dataset used to train the generative model can affect the distribution \hat{P} . To measure the bias present in generative models, recent works [8, 41] propose using statistical parity. Specifically, given a classifier $h : \mathcal{X} \rightarrow \mathcal{A}$ for the spurious attribute, the discrepancy of the generative distribution \hat{P} is defined as the L2 norm between empirical and uniform distributions [8]:

$$\sqrt{\sum_{a \in \mathcal{A}} (\mathbb{E}_{x \sim \hat{P}} [\mathbb{1}_{h(x)=a}] - 1/|\mathcal{A}|)^2} \quad (2)$$

In practice, the expectation is estimated with empirical samples. A fair generative model minimizes the discrepancy by ensuring that each attribute $a \in \mathcal{A}$ has an equal probability (uniformly distributed).

4 Debiasing Discriminative Models

It is essential for a robust classifier to evade dependence on irrelevant features present in images. This necessitates the classifier to be invariant to image backgrounds and insensitive to attributes such as race or gender. Prior research has employed datasets with target labels and spurious attributes to quantify and eliminate biases [37, 49]. However, this approach is not feasible in a zero-shot setting, where data and training are prohibitive.

4.1 Measuring Biases with Prompts

In contrast to previous approaches, our proposed method for measuring biases utilizes prompts, drawing inspiration from studies on debiasing word embeddings [6]. The use of vision-language

	CelebA		Waterbird	
	Male	Female	Land	Water
$\beta_{y=0}$	0.83	0.78	0.75	0.66
$\beta_{y=1}$	0.77	0.85	0.65	0.70

Table 1: Cosine similarity between classifier weights and spurious directions. In both datasets, the classifier weights are biased toward certain spurious attributes.

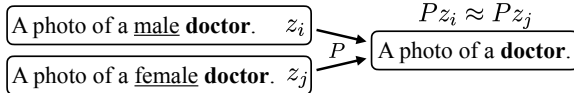


Figure 1: Calibration with Positive Pairs. Upon projecting out irrelevant features (such as gender), the embeddings of group prompts should exhibit similarity and contain only information pertaining to the target class (e.g. doctor).

contrastive training allows for the description of irrelevant features through natural language. As such, embeddings of prompts such as “a photo of a [irrelevant attribute]” can capture these spurious features in the visual embedding. Consequently, the bias of a classifier can be quantified by computing the cosine similarity between its weights and the corresponding spurious feature. Table 1 illustrates the cosine similarity between the embeddings of prompts that describe the target classes and irrelevant attributes, using two popular group robustness benchmarks: Waterbird [37] and CelebA [25]. The details of datasets and the specific prompts can be found in section 5 and appendix C.1. The results demonstrate that the classifier weights are inclined towards certain irrelevant attributes (gender or image background), implicitly implying that the classifiers are using these spurious directions to make predictions.

4.2 Debiasing via Orthogonal Projection

As the zero-shot weights can also be viewed as natural language embeddings, a straightforward approach is to follow the debiasing pipeline employed in word and sentence embeddings [6, 24]. In particular, to make the classifier invariant to these irrelevant features, we align the classifier weights with the orthogonal complement of these embeddings. Let $A \in \mathbb{R}^{d \times m}$ be a matrix whose columns are the embeddings of spurious prompts. The orthogonal projection matrix is then:

$$P_0 = I - A(A^T A)^{-1} A^T.$$

We can use the projection matrix to eliminate spurious directions in a text embedding z as $P_0 z$.

4.3 Calibrating the Projection Matrix

It is essential to acknowledge that the estimation of the irrelevant feature directions may introduce an approximation error in the projection matrix [15]. Additionally, in certain scenarios, it may be challenging to thoroughly describe the irrelevant attribute using a limited number of prompts, resulting in increased uncertainty in the projection matrix estimation. This issue is also evident in our empirical results (Table 2 and 4), where the use of orthogonal projection fails to enhance performance.

To improve the estimation of the projection matrix, we leverage *positive pairs* of prompts that are expected to have the same semantic meaning after projection. In particular, the embedding of prompts such as “a photo of a [class name] with [spurious attribute]” should only contain information about “[class name]” after projecting out the spurious information, as Figure 1 illustrates. Motivated by this intuition, we propose to regularize the difference between the projected embeddings using a set of positive pairs S :

$$\min_P \|P - P_0\|^2 + \frac{\lambda}{|S|} \sum_{(i,j) \in S} \|Pz_i - Pz_j\|^2, \quad (3)$$

where (z_i, z_j) is the embedding of pair (i, j) in S and (i, j) are prompts that describe the same class but different spurious attributes. The loss encourages the linear projection P to be invariant to the difference between (i, j) , i.e., the spurious attributes. The optimization problem has a convenient closed-form solution, as demonstrated in Lemma 4.1.

Lemma 4.1. *The minimizer of the calibration loss is*

$$P^* = P_0 \left(I + \frac{\lambda}{|S|} \sum_{(i,j) \in S} (z_i - z_j)(z_i - z_j)^T \right)^{-1}.$$

We can obtain an interpretation of the minimizer by relating it to singular value decomposition (SVD). Let $Z_{\text{diff}} \in \mathbb{R}^{d \times |\mathcal{S}|}$, where the columns of Z_{diff} enumerate the pairwise difference $z^i - z^j$ for all $(i, j) \in \mathcal{S}$. The matrix Z_{diff} defines a subspace that represents the variation in the embedding when the irrelevant feature is changed. Using Z_{diff} , the minimizer can be written as $P^* = P_0(I + \lambda' Z_{\text{diff}} Z_{\text{diff}}^T)^{-1}$, where we define $\lambda' = \lambda/|\mathcal{S}|$ to simplify the notation. Assume that the SVD of Z_{diff} is $U\Sigma V^T$. Then we have $Z_{\text{diff}} Z_{\text{diff}}^T = U\Sigma^2 U^T$. The optimal solution P^* can then be rewritten as

$$P^* = P_0(U(I + \lambda'\Sigma^2)U^T)^{-1} = P_0 \underbrace{U(I + \lambda'\Sigma^2)^{-1}U^T}_{\text{Calibration Matrix}}.$$

We can see that $U(I + \lambda'\Sigma^2)^{-1}U^T$ acts as a calibration term. Before multiplying the text embedding with the projection matrix P_0 , variation due to the change of the spurious feature, namely, the eigenvectors with large squared singular value in Z_{diff} (spurious direction) will be down-weighted due to the inverse $(I + \lambda'\Sigma^2)^{-1}$. Therefore, varying the spurious attributes should result in similar embeddings after multiplying the calibration matrix.

4.4 Relation to an Equalization Loss

Finally, we provide an equivalent form of the calibrated projection and relate it to an equalization loss. Ideally, we want each row of the classifier weight $\beta \in \mathbb{R}^{K \times d}$ to have similar cosine similarity to pairs of embeddings in \mathcal{S} . For instance, the embedding of “a photo of a doctor” should be equally similar to “a photo of a male doctor” and “a photo of a female doctor”. In this section, we will show that the optimum of the calibration loss does satisfy this criterion.

We consider the following objective for obtaining a debiased text embedding $z \in \mathbb{R}^d$ of a prompt given its initialization $z_0 \in \mathbb{R}^d$ from the text encoder:

$$\min_z \|z - z_0\|^2 + \frac{\lambda}{|\mathcal{S}|} \sum_{(i,j) \in \mathcal{S}} (z^T z_i - z^T z_j)^2. \quad (4)$$

The loss encourages the embedding z to have similar cosine similarity to embeddings in positive pairs while maintaining proximity to the initialization z_0 . Objective (4) has the same optimal solution as the calibration loss (3).

Lemma 4.2. *The minimizer of objective (4) reads*

$$z^* = \underbrace{\left(I + \frac{\lambda}{|\mathcal{S}|} \sum_{(i,j) \in \mathcal{S}} (z_i - z_j)(z_i - z_j)^T \right)^{-1}}_{\text{Calibration Matrix}} z_0$$

In particular, we have $P_0 z^ = P^* z_0$ where P^* is the minimizer of the calibration loss (3).*

Lemma 4.2 shows that the optimal solution of (4) is equivalent to multiplying the original embedding z with the calibration matrix defined before. Applying the projection P_0 to z^* leads to the same weight in Lemma 4.1. This interpretation is particularly useful in cases where the ideal solution does not lie in the middle of z_i and z_j , as will be shown in section 6 where we address biases in generative models.

The equalization objective has a similar motivation as the equalization step proposed by Bolukbasi et al. [6] in their work on removing gender bias from word embeddings. Similar to the idea of positive pairs, given a set of word embeddings that has the same semantic meaning except for gender, their approach centers these embeddings by setting them to the average embedding of the set. After centering, any word in the dictionary will be equidistant to all words in the set. However, our approach differs in that we modify the embedding of the target prompt z , rather than the embedding of positive pairs, making it more suitable for debiasing zero-shot classifiers as we are primarily concerned with the embedding of z .

5 Experiments: Discriminative Models

5.1 Group Robustness against Spurious Correlations

By following the setting of Zhang and Ré [49], we evaluate our approach on two popular benchmarks for evaluating spurious correlations, Waterbird [37] and CelebA [25]. On Waterbird, a water/land

Backbone	CLIP ResNet-50						CLIP ViT-L/14					
Dataset	Waterbird			CelebA			Waterbird			CelebA		
	WG	Avg	Gap	WG	Avg	Gap	WG	Avg	Gap	WG	Avg	Gap
<i>methods using data and labels</i>												
ERM Linear	7.9	93.5	85.6	11.9	94.7	82.8	65.9	97.6	31.7	28.3	94.7	66.4
ERM Adapter	60.8	96.0	35.2	36.1	94.2	58.1	78.4	97.8	19.4	36.7	94.2	57.5
WiSE-FT	49.8	91.0	41.2	85.6	88.6	3.0	65.9	97.6	31.7	80.0	87.4	7.4
DFR (Sub)	63.9	91.8	27.9	76.9	92.5	15.6	51.9	95.7	43.8	76.3	92.1	15.8
DFR (Up)	51.3	92.4	41.1	89.6	91.8	2.2	65.9	96.1	30.2	83.7	91.2	7.5
CA	83.7	89.4	5.7	90.0	90.7	0.7	86.9	96.2	9.3	84.6	90.4	5.8
<i>methods without data and labels</i>												
Zero-shot	39.6	77.3	37.7	75.9	82.3	6.4	45.3	84.4	39.1	72.8	87.6	14.9
Orth-Proj (Ours)	48.1	83.6	35.4	61.4	86.4	25.0	61.4	86.4	25.0	71.1	87.0	15.9
Orth-Cali (Ours)	74.0	78.7	4.7	82.2	84.4	2.2	68.8	84.5	15.7	76.1	86.2	10.1

Table 2: Group Robustness of Vision-Language Models. For each backbone, the first blocks contain methods that require data and labels, while the second blocks contain zero-shot methods. The numbers for the first block are adopted from Zhang and Ré [49]. The proposed calibration loss achieves comparable or even smaller gaps between average and worst group accuracy without the need for any data or labels.

background is a confounding factor for the waterbirds/landbirds class, while on CelebA the binary gender is the spurious feature for blond/dark hair. Therefore, both datasets contains four groups defined by the labels and the spurious attributes. As such, both datasets contain four groups defined by the labels and the spurious attributes.

We evaluate our approach against several baselines, including zero-shot classification [33], empirical risk minimization (ERM) with linear probing [23], and ERM with non-linear adapter [12]. Additionally, we also consider three recent methods designed to improve the group robustness of vision-language foundation classifiers:

- Weight Space Ensembling (WiSE-FT) [47], which trains a linear classifier first using ERM and then combines the classifier outputs with the initial zero-shot predictions;
- Deep Feature Reweighting (DFR) [22], which trains a linear probe on embeddings obtained from a pre-trained model using group-balanced data. Following Zhang and Ré [49], the group labels are replaced with zero-shot predictions;
- Contrastive Adapter (CA) [49], which trains adapters using contrastive learning to bring embeddings in the same class closer.

It is important to note that **all of the baselines** except the zero-shot classifier **require at least training data and class labels**, while our debiasing approach does not require access to any input data, labels, or group labels, which follows the principles of zero-shot learning.

We evaluate the performance of our proposed approach using two CLIP backbones: ResNet-50 [18] and ViT-L/14 [10]. The results are presented in Table 2. The results indicate that a simple application of the orthogonal projection (Orth-Proj) by itself only yields limited improvement of the worst group accuracy, whereas the calibration loss (Orth-Cali) significantly improves robustness across datasets and base models. The proposed Orth-Cali method achieves comparable or even smaller gaps between average and worst group accuracy compared to the state-of-the-art contrastive adapter [49], without the need for any data or labels. Note that the baselines generally achieve better average accuracy as they require fine-tuning on the target datasets.

	Waterbird			CelebA		
	WG	Avg	Gap	WG	Avg	Gap
$\lambda = 200$	71.8	80.8	9.0	80.7	83.9	3.2
$\lambda = 400$	72.9	79.5	6.6	81.6	84.2	2.6
$\lambda = 600$	73.5	79.2	5.7	81.9	84.3	2.4
$\lambda = 1000$	74.0	78.7	4.7	82.2	84.4	2.2

Table 3: Sensitivity to λ . We vary the weighting parameter λ and evaluate group robustness with ResNet-50 backbone.

Empirically, we found that gradually increasing the parameter λ improves the worst group accuracy and leads to a stable solution as shown in Table 3. Therefore, for all the experiments on discriminative models, we set λ to 1000 by default. To investigate the importance of orthogonal projection and calibration, we present an ablation study in Table 4. The results indicate that the calibration loss alone ($P_0 = I$) performs well on the CelebA dataset, as the spurious feature (gender) is relatively

	Waterbird			CelebA				CLIP ViT-B/32			CLIP ViT-L/14		
	WG	Avg	Gap	WG	Avg	Gap		Gen	Race	Age	Gen	Race	Age
Proj only	48.1	83.6	35.4	61.4	86.4	25.0	Zero-shot	.206	.743	.797	.206	.768	.703
Cali only	55.6	81.6	26.0	81.6	84.7	3.1	Orth-Proj	.146	.755	.635	.349	.605	.706
Proj + Cali	74.0	78.7	4.7	82.2	84.4	2.2	Orth-Cali	.102	.638	.641	.200	.461	.662

Table 4: Dissecting Orthogonal Projections. We evaluate variants of orthogonal projection with ResNet-50 backbone.

Table 5: Measuring biases on FairFace. We evaluate MaxSkew@1000 (the smaller the better) on FairFace validation set.

easy to describe with prompts. However, performance drops on the Waterbird dataset without a good initialization from the orthogonal projection. More ablation studies can also be found in Appendix D, where we demonstrate the importance of class names in positive pairs.

5.2 Debiased Information Retrieval

Fairness in text-image retrieval has gained increasing attention in recent years. Building on the work of Berg et al. [3], we propose to utilize the MaxSkew metric, introduced by Geyik et al. [14], to evaluate the level of fairness in the retrieval results. Specifically, we conduct our analysis on the FairFace dataset [21], which is specifically designed to address issues of fairness in facial recognition systems. Given a ranked list of images in response to a text query, let $r_{a,k}$ be the ratio of the top k images that are labeled with attribute a . Then MaxSkew@ k is defined as $\max_{a \in \mathcal{A}} \log \frac{r_{a,k}}{1/|\mathcal{A}|}$. It quantifies the maximal discrepancy between the ratio of top k images labeled with a specific sensitive attribute, denoted as $r_{a,k}$, and the uniform weight $1/|\mathcal{A}|$, where \mathcal{A} represents the set of sensitive attributes. The MaxSkew metric provides a useful measure of fairness in text-image retrieval systems, by assessing the degree to which the retrieval results are evenly distributed across sensitive attributes. A small MaxSkew value indicates that the distribution of retrieved images across different sensitive attributes is close to being uniform.

To measure the bias, we query the validation set of FairFace based on 10 prompts that are uncorrelated with facial expressions or sensitive attributes, e.g., “a photo of a [concept] person”, where the [concept] is a neutral concept such as evil or smart. The detailed prompts are described in Appendix C. We measure the MaxSkew based on three labeled attributes of FairFace: gender, race, and age. Table 5 shows the average MaxSkew@1000 over concepts, demonstrating that our approach significantly reduces the MaxSkew across different attributes and backbones.

6 Debiasing Generative Models

We now explore the possibility of extending the methodology developed for discriminative models to generative models. Our primary focus is on addressing social group biases, specifically gender and race discrepancy, as measured by metric (1). In particular, the main experiment is to query the generative model using profession-related prompts, specifically “a photo of a [profession]”. Empirically, the generated images were found to exhibit a strong bias towards certain gender and race, and we attempt to improve the diversity of generated images with the proposed equalization loss in this section. We also demonstrate that our approach can also address spurious correlations beyond social biases.

A Single Matrix for Comprehensive Debiasing Unlike the well-defined targets prevalent in zero-shot classification, the nature of generative models requires a more universal solution. Specifically, we seek to derive a debiasing matrix capable of accommodating any prompt. This matrix could subsequently be treated as a standardized preprocessing step, applied prior to the introduction of the embedding into the generator.

To achieve this, we optimize the equalization loss with positive pairs consisting of an enumeration of “a photo of a [attribute] [profession]” where the [attribute] is a member of the set of gender or races and the [profession] is a job title sampled from a training set. For instance, to mitigate gender bias, we adopt $\mathcal{S} = \{(\text{“a photo of a male doctor”}, \text{“a photo of a female doctor”}), \dots, (\text{“a photo of a male engineer”}, \text{“a photo of a female engineer”})\}$. By solving the calibration matrix with professions in the training set, we expect the obtained matrix can also mitigate the biases in unseen professions. Note that we optimize the equalization loss (4) without applying the initial orthogonal projection



Figure 2: Improving Gender Diversity of Stable Diffusion. We fix the random seed of initial latent noise of Stable Diffusion [36] and generate the images with the training / testing prompt “a photo of a doctor / firefighter”. The results demonstrate that applying the calibration matrix to the prompt embedding improves the balance between male and female in the generated images.

matrix P_0 . This is because our goal is to balance rather than completely eliminate biased information in the generated images.

7 Experiments: Generative Models

To evaluate the effectiveness of our approach in the context of generative models, we conducted experiments using the Stable Diffusion (SD) v2.1 framework [36]. We construct a list of professions that consists of 100 job titles with GPT-4 [31] and randomly separate them into 80 training and 20 testing professions. The complete list can be found in appendix C. In alignment with the framework proposed by Kärkkäinen and Joo [21], we consider the gender attributes of male and female, and racial attributes of White, Asian, Black, Indian, and Latino¹.

Evaluating generative models can be challenging without the use of human labels. Inspired by Cho et al. [7], we used sensitive attribute classifiers to predict the sensitive attributes of the generated images. The discrepancy, as defined in equation (2), was then calculated. In particular, we generate 100 images for each train / test profession for evaluation, resulting in 10000 images for each model. We then leverage the CLIP classifier to predict the sensitive attributes to calculate the discrepancy. An alternative to CLIP is the FairFace classifier [21]; however, we found that the domain shift between the FairFace dataset and the generated images significantly impairs its performance. The debiased and biased models share the same random seed for fair comparison. We set $\lambda = 500$ for all the experiments in this section.

7.1 Measuring the Generalization of Calibration

We first examine whether minimizing the calibration loss with training prompts can yield a calibration matrix that also works for unseen (testing) professions. In particular, we measure the average L2 difference between the projected embedding $\sum_{(i,j) \in S_{\text{test}}} \|Pz_i - Pz_j\| / |S_{\text{test}}|$ for testing prompts and show the results in Table 6. We can see that the calibration matrix successfully minimizes the difference after projection, even for unseen professions.

	Gender		Race	
	before	after	before	after
train	0.56	0.14	0.70	0.23
test	0.54	0.16	0.69	0.26

Table 6: Difference between embeddings ($\lambda = 500$).

¹It is essential to recognize gender and race are complex social constructs that cannot be simply reduced to binary or discrete categories. The choice of using binary gender and discrete race attributes in our work was primarily based on the existing literature and benchmark datasets that have commonly adopted this setting for evaluation purposes.



Figure 3: Improving Racial Diversity of Stable Diffusion. We again generate the images with Stable Diffusion. After applying the calibration matrix, the race attributes are more diverse in the generated images.

7.2 Quantitative and Qualitative Results

The results presented in Table 7 demonstrate a significant reduction in both gender and race discrepancy after debiasing. Importantly, the improvements are observed for both training and testing professions, implying that the obtained debiasing matrix can generalize beyond training prompts. To further illustrate the effectiveness of our approach, we present quantitative results for mitigating gender bias in Figure 2. By applying the calibration matrix to balance the male and female directions, the gender diversity of the generated images significantly improved. Additional examples can be found in appendix D.

Compared to gender bias, we found that addressing racial bias is a more challenging task. One source of complexity is the ambiguity of ethnicity, as individuals may identify with multiple races. Nevertheless, as Figure 3 and Table 7 demonstrate, the diversity in the output images is improved by simply debiasing the prompt embedding with the calibration matrix.

7.3 Human Evaluation

Despite the scalability, the prediction from a trained classifier could be erroneous. Therefore, we also evaluate our approach with human evaluation, where we invite annotators of different genders, races, and nationalities to label the sensitive attributes of the generated images. Details and the interface are included in appendix C.2. For human evaluation, we generate 25 images for each test profession, resulting in 500 images for each model. As Table 8 shows, our approach greatly improves the diversity of the generated images, corroborating the previous results.

7.4 Beyond Social Biases

Our approach can also be applied to address general spurious attributes beyond social biases. As an example, we draw inspiration from the WaterBird dataset [37] and debias the prompt “a photo of a wa-

		Gender	Race
Train	SD	0.472±0.225	0.485±0.160
	Ours	0.395±0.205	0.434±0.163
Test	SD	0.412±0.255	0.528±0.184
	Ours	0.354±0.253	0.455±0.169

Table 7: Discrepancy between Groups: Calibration matrix reduces the discrepancy over gender and race. The calibration matrix derived from the training set generalizes well to testing set.

		Gender	Race
SD		0.472±0.257	0.723±0.185
Ours		0.372±0.253	0.589±0.188

Table 8: Human Evaluation. We calculate the discrepancy on testing professions with human annotations. Our approach improves the diversity of Stable Diffusion by a non-trivial margin.

terbird” by using {“a photo of a [animal] with water background” and “a photo of a [animal] with land background” } as positive pairs, where we construct a list of 100 names of animals with GPT-4 [31]. As Figure 4 illustrates, our approach successfully generates images of water birds in both land and water backgrounds, whereas the original models only generated images with water background.

8 Conclusion

In this work, we present a new approach to debiasing vision-language foundation models by utilizing prompts to mitigate biases. The proposed calibrated projection effectively mitigates biases in both discriminative and generative vision-language models without any additional training or data.



Figure 4: Generation against Non-social Biases. The results demonstrate the ability of the proposed method to generate images of waterbirds in both land and water backgrounds.

Acknowledgements Thanks to Arjun Akula, Susanna Rico, Joshua Robinson, Lucy Chai, Kabir Swain, Manel Baradad, Joanna Materzynska, Shobhita Sundaram, Pei-Ling Chiang, and Yi-Yi Chu for their helpful comments and suggestions. This work was in part supported by NSF BIGDATA IIS-1741341, NSF CAREER 1553284, and NSF AI Institute TILOS. CYC is supported by an IBM PhD Fellowship.

References

- [1] Sandhini Agarwal, Gretchen Krueger, Jack Clark, Alec Radford, Jong Wook Kim, and Miles Brundage. Evaluating clip: towards characterization of broader capabilities and downstream implications. *arXiv preprint arXiv:2108.02818*, 2021.
- [2] Mohsan Alvi, Andrew Zisserman, and Christoffer Nellåker. Turning a blind eye: Explicit removal of biases and variation from deep neural network embeddings. In *Proceedings of the European Conference on Computer Vision (ECCV) Workshops*, pages 0–0, 2018.
- [3] Hugo Berg, Siobhan Mackenzie Hall, Yash Bhargat, Wonsuk Yang, Hannah Rose Kirk, Aleksandar Shtedritski, and Max Bain. A prompt array keeps the bias away: Debiasing vision-language models with adversarial learning. *arXiv preprint arXiv:2203.11933*, 2022.
- [4] Abeba Birhane, Vinay Uday Prabhu, and Emmanuel Kahembwe. Multimodal datasets: misogyny, pornography, and malignant stereotypes. *arXiv preprint arXiv:2110.01963*, 2021.
- [5] Su Lin Blodgett, Solon Barocas, Hal Daumé III, and Hanna Wallach. Language (technology) is power: A critical survey of "bias" in nlp. *arXiv preprint arXiv:2005.14050*, 2020.
- [6] Tolga Bolukbasi, Kai-Wei Chang, James Y Zou, Venkatesh Saligrama, and Adam T Kalai. Man is to computer programmer as woman is to homemaker? debiasing word embeddings. *Advances in neural information processing systems*, 29, 2016.
- [7] Jaemin Cho, Abhay Zala, and Mohit Bansal. Dall-eval: Probing the reasoning skills and social biases of text-to-image generative transformers. *arXiv preprint arXiv:2202.04053*, 2022.
- [8] Kristy Choi, Aditya Grover, Trisha Singh, Rui Shu, and Stefano Ermon. Fair generative modeling via weak supervision. In *International Conference on Machine Learning*, pages 1887–1898. PMLR, 2020.
- [9] Ching-Yao Chuang and Youssef Mroueh. Fair mixup: Fairness via interpolation. *arXiv preprint arXiv:2103.06503*, 2021.
- [10] Alexey Dosovitskiy, Lucas Beyer, Alexander Kolesnikov, Dirk Weissenborn, Xiaohua Zhai, Thomas Unterthiner, Mostafa Dehghani, Matthias Minderer, Georg Heigold, Sylvain Gelly, et al. An image is worth 16x16 words: Transformers for image recognition at scale. *arXiv preprint arXiv:2010.11929*, 2020.

- [11] Felix Friedrich, Patrick Schramowski, Manuel Brack, Lukas Struppek, Dominik Hintersdorf, Sasha Luccioni, and Kristian Kersting. Fair diffusion: Instructing text-to-image generation models on fairness. *arXiv preprint arXiv:2302.10893*, 2023.
- [12] Peng Gao, Shijie Geng, Renrui Zhang, Teli Ma, Rongyao Fang, Yongfeng Zhang, Hongsheng Li, and Yu Qiao. Clip-adapter: Better vision-language models with feature adapters. *arXiv preprint arXiv:2110.04544*, 2021.
- [13] Nikhil Garg, Londa Schiebinger, Dan Jurafsky, and James Zou. Word embeddings quantify 100 years of gender and ethnic stereotypes. *Proceedings of the National Academy of Sciences*, 115(16):E3635–E3644, 2018.
- [14] Sahin Cem Geyik, Stuart Ambler, and Krishnaram Kenthapadi. Fairness-aware ranking in search & recommendation systems with application to linkedin talent search. In *Proceedings of the 25th acm sigkdd international conference on knowledge discovery & data mining*, pages 2221–2231, 2019.
- [15] Hila Gonen and Yoav Goldberg. Lipstick on a pig: Debiasing methods cover up systematic gender biases in word embeddings but do not remove them. *arXiv preprint arXiv:1903.03862*, 2019.
- [16] Aditya Grover, Jiaming Song, Ashish Kapoor, Kenneth Tran, Alekh Agarwal, Eric J Horvitz, and Stefano Ermon. Bias correction of learned generative models using likelihood-free importance weighting. *Advances in neural information processing systems*, 32, 2019.
- [17] Melissa Hall, Laura Gustafson, Aaron Adcock, Ishan Misra, and Candace Ross. Vision-language models performing zero-shot tasks exhibit gender-based disparities. *arXiv preprint arXiv:2301.11100*, 2023.
- [18] Kaiming He, Xiangyu Zhang, Shaoqing Ren, and Jian Sun. Deep residual learning for image recognition. In *Proceedings of the IEEE conference on computer vision and pattern recognition*, pages 770–778, 2016.
- [19] Po-Sen Huang, Huan Zhang, Ray Jiang, Robert Stanforth, Johannes Welbl, Jack Rae, Vishal Maini, Dani Yogatama, and Pushmeet Kohli. Reducing sentiment bias in language models via counterfactual evaluation. *arXiv preprint arXiv:1911.03064*, 2019.
- [20] Pavel Izmailov, Polina Kirichenko, Nate Gruver, and Andrew Gordon Wilson. On feature learning in the presence of spurious correlations. *arXiv preprint arXiv:2210.11369*, 2022.
- [21] Kimmo Kärkkäinen and Jungseock Joo. Fairface: Face attribute dataset for balanced race, gender, and age. *arXiv preprint arXiv:1908.04913*, 2019.
- [22] Polina Kirichenko, Pavel Izmailov, and Andrew Gordon Wilson. Last layer re-training is sufficient for robustness to spurious correlations. *arXiv preprint arXiv:2204.02937*, 2022.
- [23] Ananya Kumar, Aditi Raghunathan, Robbie Jones, Tengyu Ma, and Percy Liang. Fine-tuning can distort pretrained features and underperform out-of-distribution. *arXiv preprint arXiv:2202.10054*, 2022.
- [24] Paul Pu Liang, Irene Mengze Li, Emily Zheng, Yao Chong Lim, Ruslan Salakhutdinov, and Louis-Philippe Morency. Towards debiasing sentence representations. *arXiv preprint arXiv:2007.08100*, 2020.
- [25] Ziwei Liu, Ping Luo, Xiaogang Wang, and Xiaoou Tang. Deep learning face attributes in the wild. In *Proceedings of the IEEE international conference on computer vision*, pages 3730–3738, 2015.
- [26] David Madras, Elliot Creager, Toniann Pitassi, and Richard Zemel. Learning adversarially fair and transferable representations. *International Conference on Machine Learning*, 2018.
- [27] Thomas Manzini, Yao Chong Lim, Yulia Tsvetkov, and Alan W Black. Black is to criminal as caucasian is to police: Detecting and removing multiclass bias in word embeddings. *arXiv preprint arXiv:1904.04047*, 2019.

- [28] Ninareh Mehrabi, Fred Morstatter, Nripsuta Saxena, Kristina Lerman, and Aram Galstyan. A survey on bias and fairness in machine learning. *ACM Computing Surveys (CSUR)*, 54(6):1–35, 2021.
- [29] P Mishkin, L Ahmad, M Brundage, G Krueger, and G Sastry. Dall· e 2 preview-risks and limitations. *Noudettu*, 28:2022, 2022.
- [30] Moin Nadeem, Anna Bethke, and Siva Reddy. Stereoset: Measuring stereotypical bias in pretrained language models. *arXiv preprint arXiv:2004.09456*, 2020.
- [31] OpenAI. Gpt-4 technical report. *arXiv*, 2023.
- [32] Otávio Parraga, Martin D More, Christian M Oliveira, Nathan S Gavenski, Lucas S Kupssinski, Adilson Medronha, Luis V Moura, Gabriel S Simões, and Rodrigo C Barros. Debiasing methods for fairer neural models in vision and language research: A survey. *arXiv preprint arXiv:2211.05617*, 2022.
- [33] Alec Radford, Jong Wook Kim, Chris Hallacy, Aditya Ramesh, Gabriel Goh, Sandhini Agarwal, Girish Sastry, Amanda Askell, Pamela Mishkin, Jack Clark, et al. Learning transferable visual models from natural language supervision. In *International Conference on Machine Learning*, pages 8748–8763. PMLR, 2021.
- [34] Vikram V Ramaswamy, Sunnie SY Kim, and Olga Russakovsky. Fair attribute classification through latent space de-biasing. In *Proceedings of the IEEE/CVF conference on computer vision and pattern recognition*, pages 9301–9310, 2021.
- [35] Aditya Ramesh, Prafulla Dhariwal, Alex Nichol, Casey Chu, and Mark Chen. Hierarchical text-conditional image generation with clip latents. *arXiv preprint arXiv:2204.06125*, 2022.
- [36] Robin Rombach, Andreas Blattmann, Dominik Lorenz, Patrick Esser, and Björn Ommer. High-resolution image synthesis with latent diffusion models. In *Proceedings of the IEEE/CVF Conference on Computer Vision and Pattern Recognition*, pages 10684–10695, 2022.
- [37] Shiori Sagawa, Pang Wei Koh, Tatsunori B Hashimoto, and Percy Liang. Distributionally robust neural networks for group shifts: On the importance of regularization for worst-case generalization. *arXiv preprint arXiv:1911.08731*, 2019.
- [38] Chitwan Saharia, William Chan, Saurabh Saxena, Lala Li, Jay Whang, Emily Denton, Seyed Kamyar Seyed Ghasemipour, Burcu Karagol Ayan, S Sara Mahdavi, Rapha Gontijo Lopes, et al. Photorealistic text-to-image diffusion models with deep language understanding. *arXiv preprint arXiv:2205.11487*, 2022.
- [39] Ashish Seth, Mayur Hemani, and Chirag Agarwal. Dear: Debiasing vision-language models with additive residuals. *arXiv preprint arXiv:2303.10431*, 2023.
- [40] Tony Sun, Andrew Gaut, Shirlyn Tang, Yuxin Huang, Mai ElSherief, Jieyu Zhao, Diba Mirza, Elizabeth Belding, Kai-Wei Chang, and William Yang Wang. Mitigating gender bias in natural language processing: Literature review. *arXiv preprint arXiv:1906.08976*, 2019.
- [41] Christopher TH Teo and Ngai-Man Cheung. Measuring fairness in generative models. *arXiv preprint arXiv:2107.07754*, 2021.
- [42] Jialu Wang, Yang Liu, and Xin Eric Wang. Are gender-neutral queries really gender-neutral? mitigating gender bias in image search. *arXiv preprint arXiv:2109.05433*, 2021.
- [43] Mei Wang and Weihong Deng. Mitigating bias in face recognition using skewness-aware reinforcement learning. In *Proceedings of the IEEE/CVF conference on computer vision and pattern recognition*, pages 9322–9331, 2020.
- [44] Mei Wang, Weihong Deng, Jiani Hu, Xunqiang Tao, and Yaohai Huang. Racial faces in the wild: Reducing racial bias by information maximization adaptation network. In *Proceedings of the IEEE/CVF international conference on computer vision*, pages 692–702, 2019.

- [45] Zeyu Wang, Klint Qinami, Ioannis Christos Karakozis, Kyle Genova, Prem Nair, Kenji Hata, and Olga Russakovsky. Towards fairness in visual recognition: Effective strategies for bias mitigation. In *Proceedings of the IEEE/CVF conference on computer vision and pattern recognition*, pages 8919–8928, 2020.
- [46] Laura Weidinger, John Mellor, Maribeth Rauh, Conor Griffin, Jonathan Uesato, Po-Sen Huang, Myra Cheng, Mia Glaese, Borja Balle, Atoosa Kasirzadeh, et al. Ethical and social risks of harm from language models. *arXiv preprint arXiv:2112.04359*, 2021.
- [47] Mitchell Wortsman, Gabriel Ilharco, Jong Wook Kim, Mike Li, Simon Kornblith, Rebecca Roelofs, Raphael Gontijo Lopes, Hannaneh Hajishirzi, Ali Farhadi, Hongseok Namkoong, et al. Robust fine-tuning of zero-shot models. In *Proceedings of the IEEE/CVF Conference on Computer Vision and Pattern Recognition*, pages 7959–7971, 2022.
- [48] Depeng Xu, Shuhan Yuan, Lu Zhang, and Xintao Wu. Fairgan: Fairness-aware generative adversarial networks. In *2018 IEEE International Conference on Big Data (Big Data)*, pages 570–575. IEEE, 2018.
- [49] Michael Zhang and Christopher Ré. Contrastive adapters for foundation model group robustness. *arXiv preprint arXiv:2207.07180*, 2022.
- [50] Jieyu Zhao, Tianlu Wang, Mark Yatskar, Vicente Ordonez, and Kai-Wei Chang. Men also like shopping: Reducing gender bias amplification using corpus-level constraints. *arXiv preprint arXiv:1707.09457*, 2017.
- [51] Jieyu Zhao, Tianlu Wang, Mark Yatskar, Ryan Cotterell, Vicente Ordonez, and Kai-Wei Chang. Gender bias in contextualized word embeddings. *arXiv preprint arXiv:1904.03310*, 2019.

A Broader Impact

The development and implementation of debiasing techniques in vision and language models has the potential to significantly impact a wide range of industries and applications. By reducing the biases in the models, they will be better able to accurately recognize and understand diverse individuals and groups, leading to more fair and equitable decision-making in fields such as education, employment, and law enforcement. Nevertheless, our approach also has limitations. For instance, the proposed debiased technique for generative models does not work for certain classes or biases. Despite the limitations, our work on debiasing vision and language models is a crucial step towards creating more inclusive and fair technology for all.

B Proof

B.1 Lemma 4.1

Proof. We will leverage the first order optimality criteria to derive the solution.

$$\min_P \|P - P_0\|^2 + \frac{\lambda}{|\mathcal{S}|} \sum_{(i,j) \in \mathcal{S}} \|Pz_i - Pz_j\|^2$$

The loss can be written as

$$\begin{aligned} \mathcal{L}(P) &= \frac{\lambda}{|\mathcal{S}|} (Pz_i - Pz_j)^T (Pz_i - Pz_j) + (P - P_0)^T (P - P_0) \\ &= \frac{\lambda}{|\mathcal{S}|} (z_i^T P^T P z_i + z_j^T P^T P z_j - z_i^T P^T P z_j - z_j^T P^T P z_i) + (P^T P + P_0^T P_0 - P_0^T P - P^T P_0) \end{aligned}$$

Setting the derivate w.r.t. P to zero yields:

$$\begin{aligned} \frac{\partial \mathcal{L}(P)}{\partial P} &= \frac{\lambda}{|\mathcal{S}|} \sum_{(i,j) \in \mathcal{S}} 2(Pz_i z_i^T + Pz_j z_j^T - Pz_i z_j^T - Pz_j z_i^T) + (2P - 2P_0) = 0 \\ P(I + \frac{\lambda}{|\mathcal{S}|} \sum_{(i,j) \in \mathcal{S}} (z_i z_i^T + z_j z_j^T - z_i z_j^T - z_j z_i^T)) &= P_0 \\ P &= P_0 (I + \frac{\lambda}{|\mathcal{S}|} \sum_{(i,j) \in \mathcal{S}} (z_i z_i^T + z_j z_j^T - z_i z_j^T - z_j z_i^T))^{-1} \\ &= P_0 \left(I + \frac{\lambda}{|\mathcal{S}|} \sum_{(i,j) \in \mathcal{S}} (z_i - z_j)(z_i - z_j)^T \right)^{-1} \end{aligned}$$

One can also rewrite the objective as

$$\begin{aligned} \min_P \|P - P_0\|^2 + \frac{\lambda}{|\mathcal{S}|} \sum_{(i,j) \in \mathcal{S}} \|P(z_i - z_j)\|^2 \\ = \min_P \|P - P_0\|^2 + \frac{\lambda}{|\mathcal{S}|} \|PZ_{\text{diff}}\|^2 \end{aligned}$$

We then have

$$\begin{aligned} \frac{\partial \mathcal{L}(P)}{\partial P} &= 2(P - P_0) + 2 \frac{\lambda}{|\mathcal{S}|} PZ_{\text{diff}}Z_{\text{diff}}^T = 0 \\ P(I + \frac{\lambda}{|\mathcal{S}|} Z_{\text{diff}}Z_{\text{diff}}^T) &= P_0 \\ P &= P_0 (I + \frac{\lambda}{|\mathcal{S}|} Z_{\text{diff}}Z_{\text{diff}}^T)^{-1}. \end{aligned}$$

Note that two optimums are equivalent, where the second one is simply the matrix form of the first. \square

B.2 Lemma 4.2

Proof. Similarly, the objective can be rewritten as

$$\begin{aligned} & \min_z \|z - z_0\|^2 + \frac{\lambda}{|\mathcal{S}|} \sum_{(i,j) \in \mathcal{S}} (z^T(z_i - z_j))^2 \\ & = \min_z \|z - z_0\|^2 + \frac{\lambda}{|\mathcal{S}|} \|z^T Z_{\text{diff}}\|^2. \end{aligned}$$

The derivative is:

$$\begin{aligned} \frac{\partial \mathcal{L}(z)}{\partial z} &= 2z - 2z_0 + 2 \frac{\lambda}{|\mathcal{S}|} Z_{\text{diff}} Z_{\text{diff}}^T z = 0 \\ z &= \left(I + \frac{\lambda}{|\mathcal{S}|} Z_{\text{diff}} Z_{\text{diff}}^T \right)^{-1} z_0 \\ &= \left(I + \frac{\lambda}{|\mathcal{S}|} \sum_{(i,j) \in \mathcal{S}} (z_i - z_j)(z_i - z_j)^T \right)^{-1} z_0 \end{aligned}$$

□

	Class Prompt
$y = 0$	This is a picture of a landbird.
$y = 1$	This is a picture of a waterbird.
	Spurious Prompt
	This is a land background. This is a picture of a forest. This is a picture of a mountain. This is a picture of a wood. This is a water background. This is a picture of an ocean. This is a picture of a beach. This is a picture of a port.
	Positive Pairs
enumerate of	This is a picture of a landbird with land background. This is a picture of a landbird with water background. This is a picture of a landbird in the ocean This is a picture of a landbird in the water. This is a picture of a landbird in the forest.
enumerate of	This is a picture of a waterbird with land background. This is a picture of a waterbird with water background. This is a picture of a waterbird in the ocean This is a picture of a waterbird in the water. This is a picture of a waterbird in the forest.

Table 9: Prompts for WaterBird Dataset. The spurious prompts are sentences that describe the spurious features, that is, the background of the images. In addition to keywords such as land/water background, we further include terms that describe similar concepts, such as forest or ocean. The positive pairs consist of sentences that describe the same type of bird (landbird/waterbird), while phrases that describe the background are appended afterward.

C Experiment Details

C.1 Prompts

In this section, we provide the exact prompt we use for all the experiments in the paper in Table 9, 10, 11, 12.

C.2 Human Evaluation

We generate 100 images for each profession for evaluation. Therefore, there are 1500 images for each model in total. The random seed is fixed for the original and debiased Stable Diffusion models. In particular, automatic evaluation and human evaluation adopt the same set of images for fair

Class Prompt	
$y = 0$	A photo of a celebrity with dark hair.
$y = 1$	A photo of a celebrity with blond hair.
Spurious Prompt	
	A photo of a male. A photo of a male celebrity. A photo of a man. A photo of a female. A photo of a female celebrity. A photo of a woman.
Positive Pairs	
	(A photo of a male celebrity with dark hair., A photo of a female celebrity with dark hair.) (A photo of a male celebrity with blond hair., A photo of a female celebrity with blond hair.)

Table 10: Prompts for CelebA Dataset. We found two positive pairs are sufficient to mitigate the biases for CelebA dataset.

Prompt:	A photo of a [CONCEPT] person.
CONCEPT:	good, evil, smart, dumb, attractive, unattractive, lawful, criminal, friendly, unfriendly

Table 11: Prompts for text-image retrieval on FairFace Dataset. We adopt the 10 training concepts from [3] to construct the prompts for FairFace. These concepts are irrelevant to gender, race, or age, which makes them suitable for evaluating the model biases.

comparison. The interface for human evaluation is shown in Figure 5. Note that some generated images might be corrupted, or do not even contain humans. In this case, the annotators can click 3 or 6 to indicate that the current image is not identifiable. We remove these images while calculating the discrepancy.

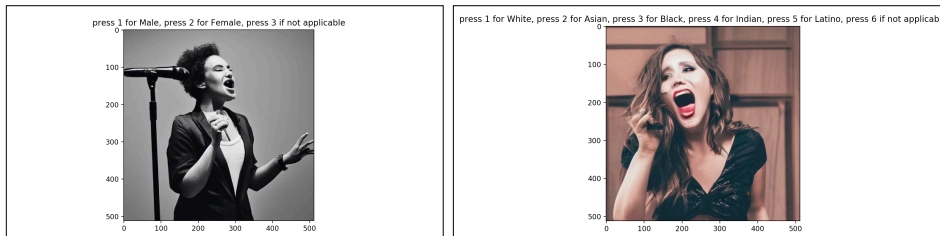


Figure 5: Interface for human evaluation. We construct a simple labeling script for the annotator to easily label the sensitive attributes. Once they select the label, the program will ask whether they are sure about the answer. One can reselect the answer or press “enter” to switch to the next image.

D More Experiment Results

D.1 Importance of Class Name in Positive Pairs

In this section, we study the importance of class names in the positive pairs. In particular, instead of using “a photo of a [class name] with [spurious attribute]”, we instead use “a photo of a [spurious attribute]” to estimate the calibration matrix. The results are shown in Table 13. We can see that the performance significantly drops after removing the class name from the prompt, emphasizing the importance of class-conditioned prompts.

D.2 More Samples from Biased and Debiased Generative Models

In this section, we show more generated images from Stable Diffusion 2.1 to provide a qualitative experiment. We can see that the proposed debiasing approach significantly improves the diversity across training and testing professions as as Figure 6, 7, 9 and 10 show. Nevertheless, there are also failure cases, where both our approach and the original model fail. For instance, biased and debiased

GENDER:	A photo of a male [profession]. A photo of a female [profession].
RACE:	A photo of a white [profession]. A photo of a black [profession]. A photo of an Asian [profession]. A photo of an Indian [profession]. A photo of a Latino [profession].

Table 12: Prompts for debiasing generative models. We simply use prompts that describe the gender and race attribute as prompts, where we avoid using ambiguous terms such as white and black as the model could wrongly interpret it as the color of the photo.

	Waterbird			CelebA		
	WG	Avg	Gap	WG	Avg	Gap
Class-Agnostic	57.5	81.4	23.9	52.8	85.2	32.4
Class-Conditioned	74.0	78.7	4.7	82.2	84.4	2.2

Table 13: Importance of target classes in the positive pairs. Removing [class name] in the positive pairs significantly degenerate the robustness of the zero-shot models.

models fail to generate females for many engineer-related professions such as carpenter as Figure 8 shows.



Figure 6: Generation against Gender Bias on Training Set. After debiasing, we can see that the gender diversity of Stable Diffusion greatly improves.



Figure 7: Generation against Gender Bias on Testing Set. We can see that by applying the calibration matrix, the gender distributions are more balanced.



Figure 8: Failure Case for Generation against Gender Bias. There are also failure cases, where both our approach and the original model fail. For instance, biased and debiased models fail to generate females for professions such as carpenter and builders.

Train	Actor, Architect, Audiologist, Author, Baker, Barber, Blacksmith, Bricklayer Bus Driver, Butcher, Chef, Chemist, Cleaner, Coach, Comedian, Computer Programmer Construction Worker, Consultant, Counselor, Dancer, Dentist, Designer, Dietitian, DJ Doctor, Driver, Economist, Electrician, Engineer, Entrepreneur, Farmer, Florist Graphic Designer, Hairdresser, Historian, Journalist, Judge, Lawyer, Librarian, Magician Makeup Artist, Mathematician, Marine Biologist, Mechanic, Model, Musician, Nanny, Nurse Optician, Painter, Pastry Chef, Pediatrician, Photographer, Plumber, Police Officer, Politician Professor, Psychologist, Real Estate Agent, Receptionist, Recruiter, Researcher, Sailor, Salesperson Surveyor, Singer, Social Worker, Software Developer, Statistician, Surgeon, Teacher, Technician Therapist, Tour Guide, Translator, Vet, Videographer, Waiter, Writer, Zoologist
Test	Accountant, Astronaut, Biologist, Carpenter, Civil Engineer, Clerk, Detective Editor, Firefighter, Interpreter, Manager, Nutritionist, Paramedic, Pharmacist Physicist, Pilot, Reporter, Security Guard, Scientist, Web Developer

Table 14: 100 Training and Testing Professions. We use GPT-4 to list 100 job titles to form our training and testing set. The similar approach can also be extended to other debiasing tasks by querying large language models.



Figure 9: Generation against Race Bias on Training Set. We can observe a clear difference before and after debiasing, where the diversity is improved after debiasing.



Figure 10: Generation against Race Bias on Testing Set. We can again see that the diversity is improved after debising even for unseen classes.

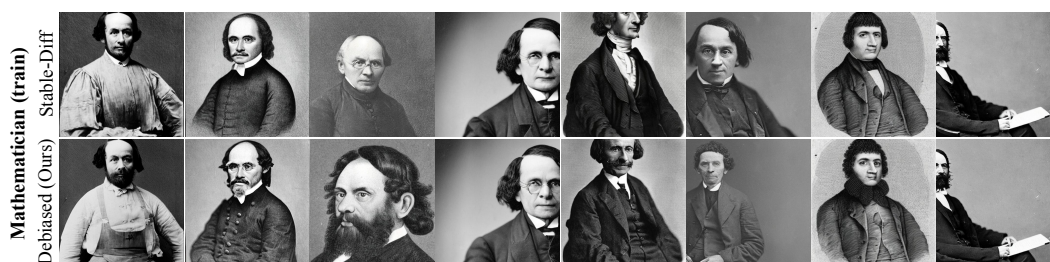


Figure 11: Failure Case for Generation against Racial Bias. For certain classes that are highly correlated with historical figures such as mathematicians, our approach does not improve the diversity a lot due to the strong biases from the data.